Determination of an Effective Trace Gas Mixing Height by Differential Optical Absorption Spectroscopy (DOAS)

B.Zhou[1], S.N.Yang[1], S.S. Wang[1], T.Wagner[2]

[1]Department of Environmental Science and Engineering, Fudan University, Shanghai, China

[2] Max Planck Institute for Chemistry, Mainz, Germany

Abstract:

A new method for the determination of the Mixing layer Height (MH) by the DOAS technique is proposed in this article. The MH can be retrieved by combination of active DOAS and passive DOAS observations of atmospheric trace gases; here we focus on observations of NO_2. Because our observations are sensitive to the vertical distribution of trace gases, we refer to the retrieved layer height as an 'effective trace gas mixing height' (ETMH). By analyzing trace gas observations in Shanghai over one year (1017 hourly means in 93 days in 2007), the retrieved ETMH was found to range between 0.1km and 2.8km (average is 0.78km); more than 90% of the measurements yield an ETMH between 0.2km and 2.0km. The seasonal and diurnal variation of the ETMH shows good agreement with mixing layer heights derived from meteorological observations. We investigated the relationship of the derived ETMH to temperature and wind speed and found correlation coefficients of 0.65 and 0.37, respectively. Also the wind direction has an impact on the measurement to some extent. Especially in cases when the air flow comes from highly polluted areas and the atmospheric lifetime of NO_2 is long (e.g. in winter), the NO_2 concentration at high altitudes over the measurement site can be enhanced, which leads to an overestimation of the ETMH. Enhanced NO_2 concentrations in the free atmosphere and heterogeneity within the mixing layer can cause additional uncertainties.

1 Introduction

Pollutants emitted into the atmospheric boundary layer are dispersed horizontally and vertically through atmospheric turbulence and convection, and finally can become completely mixed over this layer that is widely known as "mixing layer". Mixing height (MH) has a close relation to meteorological conditions, and meanwhile is a key input parameter to many air quality forecast models. MH determines the volume available for the dispersion of pollutants, so it is of particular importance in the prediction models of pollutants concentration [Seibert et al.,2000]. However, the MH is not a meteorological parameter that can be directly measured, and moreover the determination and assessment of it is still difficult.

There are two main approaches available for the estimation of MH. One is through analyzing profiles of meteorological parameters, such as temperature, pressure, humidity, and aerosol, and the profiles are attained with remote sensing techniques such as Radiosoundings, tethered balloon, mast, doppler weather radar/wind profiler, Lidar, and Sodar. MH could also be retrieved by analyzing temperature and pressure profiles from temperature and pressure sensors on commercial planes. Each method has its own advantages and disadvantages, because they can not give attention to all the aspects such as observing range, temporal and spatial resolution, measurement precision, instrument and operation cost [Seibert et al.,2000].

Fund Program: supported by "863 project", No: 2006AA06Z417 and NSFC, No:40975076
Correspondence to Bin Zhou, binzhou@fudan.edu.cn

The second approach makes use of models based on meteorological data. The first method can provide high temporal and spatial resolution information on the MH. Although widely used, the latter may entail uncertainties in the estimation of MH as discussed by certain authors [Berman et al, 1997; M. A. García , 2007]. Berman et al. (1997) found mixing depths obtained from CALMET and MIXEMUP models for nine clear days, were in good agreement with estimates derived from a 915-MHZ radar profiler, but mixing height from RAMMET-X model displayed considerably less diurnal variation. Good statistical agreement of early afternoon mixing heights derived from DIAL and those obtained from the Lagrangian HYSPLIT model, but a relatively weak relationship in the morning and night time, have been presented by Garíca et al. (M. A. García ,2007).

In this study we introduce a new technique for the estimation of the MH, which is directly related to the mixing processes of pollutants. The method is based on a combination of active and passive differential optical absorption spectroscopy (DOAS) observations of NO_2 (also other trace gases could be used). Because our observations are sensitive to the vertical distribution of trace gases, we refer to the retrieved layer height as an 'effective trace gas mixing height' (ETMH).

Since introduced in the 1970s [Perner and Platt, 1979; Noxon,1975; Platt, 1994; Evangelisti et al., 1995; Solomon, et al, 1999], DOAS method has been improved rapidly and is mainly applied in atmospheric research. The DOAS technique is based on the absorption of ultraviolet (UV) and visible light along specific light paths by atmospheric molecules. Passive DOAS observations typically use the scattered sun light as light source, and vertically integrated trace gas concentrations are usually retrieved. Recently, Chen [Chen et al., 2009] introduced a detailed method for the determination of the vertically integrated tropospheric NO_2 concentration from passive DOAS observations of zenith scattered light. Active DOAS with artificial light sources could be used to measure the average surface concentrations of trace gases.

The DOAS technique has been developed to measure many atmospheric trace gases, such as O_3, NO_2, HONO, SO_2, CS_2, BrO, IO, OClO and more than 30 kinds of hydrocarbons [FEBO et al.,1996; Vandaele et al.,2005; Hönninger et al.,2002; Kourtidis et al., 2000; Bruns et al., 2006, Platt and Stutz, 2008]. HONO, OH, NO_3, BrO, ClO in the troposphere and OClO, BrO in the stratosphere were first measured by DOAS method, the measurement precision substantially increased during recent years [Zhou et al., 2002; Qi et al.,2002].

2 method

2.1 Experimental

Determination of the ETMH based on the DOAS technique by combination of active DOAS and passive DOAS could be educed by analyzing the integrated NO_2 concentrations, respectively retrieved by active DOAS and passive DOAS.

The light source of passive DOAS is the incoming solar irradiation. The receiving telescope directed to zenith sky and receives scattered solar light. Since scattered light passes through the whole atmosphere, this method provides information on the total NO_2 column density in atmosphere. After subtracting the stratospheric NO_2 column density and correcting for light path effects, the vertical column density (VCD, the vertically integrated concentration) in the troposphere can be determined [Chen et al., 2009]. This method can be applied with good accuracy especially to observations in polluted regions. An active DOAS instrument observes light

from an artificial light source over a horizontal distance. Usually the light source is at the same location as the receiver and a retro-reflector that is placed at certain distance, folds the beam back to transmitting/receiving telescope. The light transfers a double distance between transmitting/receiving telescope and retro-reflector, and thus active DOAS offers the possibility to measure the integrated concentration of air pollutants in the lower atmosphere [Platt et al. 1994,2008; Noxon 1975; Zhou et al. 2005]. Dividing the integrated concentration by the length of the absorption path yields the average trace gas concentration along the optical path,

Figure 1 shows the measurement site, passive DOAS and transmit telescope of active DOAS are in the campus of Fudan University (31.3_ N, 121.5_ E), Shanghai, China, which is located in the north-east of Shanghai, nearby the middle cycle viaduct. Both DOAS systems were set on the roof of #4 teaching building which is nearly in the middle of the campus, light beam of active DOAS (yellow arrow in figure 1) is totally within the campus without cross of any road, it's about 20m above ground and about 250m to middle cycle (Handan Road), average distance of light beam to Guoding Road is about 300m, which is to the east of the beam and nearly perpendicular to it, in the north, there is a Wuchuan Road, which is about 400m to light beam, there is not any road in the west of measurement site until about 1500m away.

Near the measurement site, there is not any point source of NO2, around this area NO2 mainly comes from vehicle emission. because the roads are around the campus, so in middle point of the light beam (about the middle of campus), NO2 mixed well relatively to roadside.

The instrument of passive DOAS mounted on the top roof of the building comprises three parts, including a telescope, a spectrometer and a PC. The scattered sunlight is received by the telescope with 46mm diameter and 300mm focal length, and fed to spectrometer via a quartz fiber. The HR4000 high resolution fiber optic spectrometer (Ocean Optics, Inc.) is used to acquire UV-visible zenith-sky spectra with a 1200 grooves/mm grating and a 100μm wide entrance slit, which yields a full-width half-maximum (FWHM) resolution of about 0.73 nm. The detector is a linear CCD array with 3648 pixels (each 8μm×200μm). A PC controls the automatic measurements and stores the spectra. The NO2 column densities are retrieved by means of Differential Optical Absorption Spectroscopy (DOAS) (Platt, 1994), using the spectral region between 434 nm and 462 nm. The WinDOAS-software (Fayt and Roozendael, 2001) is applied to analyze the zenith-sky spectra. The cross sections of NO2 (Burrows et al., 1998), O3 (Burrows et al., 1999a), O4 (Greenblatt et al., 1990), and H2O from HITRAN (Rothman, 1998) are taken into account in the retrieving process. For details about this, please seeing Chen et al (2009).

Long-path active DOAS instrument was installed at the same location as the zenith-sky instrument. Detailed description of the instrument can be found in Yu et al. (2004). In short, the collimated beam of white light from a 150WXe short-arc lamp is transmitted by a co-axial telescope to the open atmosphere and folded back into the telescope by an array of quartz corner cube retroreflectors, which was mounted at a distance of 507m east of the experimental building and the same altitude as the telescope. Led by a quartz fiber, the light enters a spectrometer. Spectra in a wavelength range of 372–444 nm are recorded by a Czerny-Turner spectrograph with a focal length of 0.3 m, and detected by a 1024-pixel photodiode array detector cooled to −15_ C. With a fixed number of 20 scans (with an individual exposure time from 5 to 30 s), the average time resolution is about 4 min, which is similar to that of the zenith-sky measurements. The

average NO2 concentrations along the optical path are analyzed using the DOASIS software package (Kraus, 2001) in the spectral region of 424–435 nm, with the cross sections of NO2 (Burrows et al., 1998) and O3 (Burrows et al., 1999a) at 293 K, as well as the "background Fraunhofer structure" induced by the scattered sunlight received by the telescope (Zhou et al., 2005) taken into account. The retrieved amounts are taken as the NO2 surface concentrations at the experimental site.

2.2 Calculation of the effective trace gas mixing height

The basic assumption of our new technique for the determination of the ETMH is that the NO_2 is completely mixed in mixing layer and decreased to zero rapidly above mixing layer.

Vertical distribution of NO2 within mixing layer is the key point of measurement method, there are many factors that can impact NO2 mixing, especially the source of NO2, if the measurement site is far away from source, it can be accepted that NO2 mixes well in mixing layer. Jochen Stutz,(Jochen Stutz,2004) studied the distribution of NO2 near the ground at the La Porte Municipal Airport 30km ENE of the city center of Huston, TX, and nearby heavy industrialized ship channel area, with multi-beam DOAS, in-suit measurement shows no special profile of NO2 below 120m was found during day time. Jochen Stutz's research result(Stutz 2006) in Phoenix's urban area also shows the gradients of NO2 distribution gradually disappeared after the onset of convective mixing. Although our experiment setup is more closer to the center of city than Jochen Stutz experiment, but vehicle emission is the mainly NO2 source of both shanghai and Huston, and both experiments are close to line source of NO2(road and industrialized ship channel area) so Jochen Stutz's study can be used to support our assumption.

For simplicity, then we can assume that the NO_2 concentration is constant within the MH and zero above. Then $N_{LP\text{-}DOAS}$ retrieved from active DOAS and VCD_{ETMH} retrieved from passive DOAS are directly connected via the ETMH, which can be obtained by the following formula:

$$ETMH = \frac{VCD_{ETMH}}{N_{lp-DOAS}} \cdots\cdots\cdots\cdots\cdots\cdots (1)$$

The following example illustrates how to calculate the ETMH with this method. Fig. 2 shows a comparison between results from active DOAS and passive DOAS in 9, Juen, 2007, active DOAS data has been converted into VCD_{ETMH} through multiplying by assumed ETMH. In Fig. 2a, the ETMH is assumed as 0.3km. It is found that the result of active DOAS is close to that from the passive DOAS at 8:00 and from 16:00 to 17:00. Thus it can be said that the observations are in agreement with an ETMH of 0.3km at these times. Fig. 2b and 2c show similar comparisons for assumed ETMH of 0.6km and 0.8km, respectively. Good agreement with the VCD_{EMTH} is found for other periods of the day under the corresponding assumption of ETMH. Fig. 2d is the diurnal variation of ETMH calculated by the assumption in this particular day.

NO2 in free troposphere can effect the retrieving of ETMH, but by comparison with NO2 in mixing layer, the concentration of NO2 in free troposphere is very low, so the effect can be accepted for most case, because the NO2 is always high in megacity. For more detail of this, please see errors discussion in Sect. 5.

The above analysis confirms our basic assumptions, and yields results for the diurnal variation of the ETMH which are in general agreement with expectations.

It should be noted that instead of assuming a vertically constant trace gas concentration, a constant mixing ratio would be more realistic. However, for simplicity we chose a constant concentration in this first study. Since the boundary layer is usually below 2 km, the resulting errors are small, and probably usually smaller than other uncertainties. The method can in principle easily be extended using the assumption of vertically constant mixing ratio.

3 Results

To reduce the possible influence of clouds on the results of passive DOAS, only observations for mainly cloud free conditions were selected. The selection was performed according to the simultaneously observed O_4 absorptions, those days when observed daily variation of O_4 slant column density are U-shape were selected (Chen et al. [2009]).

Experiment is paused in July and August because of school vacation. As a result, there are valid data for 93 days during the whole year. Table 1 shows the distribution of measurement days in different months. According to weather condition and season, the experiment is operated from 5:00 to 18:00 every day. In total 1017 data points of hourly averages are obtained during that period. From the hourly averaged data monthly averages (Fig. 3, 4) are calculated. Except the values in January, both the seasonal and diurnal variation of the ETMH shows the expected dependence: low values occur in winter and in the morning as well as high values in summer and at noon and afternoon.

In Fig. 5 Monthly average of passive DOAS and active DOAS in 2007 were showed, it could be seen both measurements have high concentration in winter and low concentration in summer, because of the lifetime of NO2 in atmosphere.The high values of ETMH in January are probably caused by the long lifetime of NO_x in the troposphere during winter. Under such conditions, local measurements can be strongly influenced by emissions from distant sources. Since the method relies on the assumption of rapid mixing of local emissions, measurement results retrieved under such conditions have to be treated with care (for more details see section 4.3).

Due to limited space, it is impossible to illustrate every day's data. We will systematically discuss them in the next section.

the red line B in Fig.4 is Yang's (Yang, 2006) observation in shanghai, for detail of this, please see section 4.4.

4 Discussion

Mixing layer height is governed by many factors and follows a systematic seasonal variation. Meteorological parameters strongly affect the MH, especially surface temperature, wind speed, and wind direction. In this section we investigate the correlation between meteorological parameters and the ETMH.

4.1 Correlation between the ETMH and surface temperature

The variation of surface temperature controls the occurrence of atmospheric convection, so surface temperature changes have a strong effect on the MH. This relationship is well

demonstrated for the observations from 11 May 2007(see Fig. 6). It is expected that surface temperature should have the strongest effect in summer, when the solar irradiation is strongest and days are longest in the northern hemisphere. This expectation is broadly confirmed by the results shown in table 2. The correlation coefficients between the ETMH and surface temperatures are highest in autumn and summer and smallest in winter and spring.

. The monthly variation of the correlation coefficients between the ETMH and temperature is also presented in Fig 7. It's a box figure, each box represents each month, where lower and higher boundaries are the 25 and 75 percentiles. The median value and the mean concentrations are respectively the solid lines and hollow squares. The low and high external lines represent the 90 and 10 percentiles while the maximum and minimum values are marked with stars outside the boxes. This graph gives more details of the data.

It can be seen in Fig 7, that the range of means is between 0.4 and 0.84, the lowest mean occurs in December, when the minimum is -0.818, much less than other data of this month. But if we pay attention to the median, it can be found that the range is only from about 0.51 to 0.83. The lowest median appears in January, while, the highest is in September (in January and December, the median is close to the lower boundaries of the boxes). It should be mentioned that, "because there are too little data in March, June and October(just 2 days met data can be used), no median could be found in Figure 7 of those months.

In January and February, the correlation between the ETMH and temperature is a little bit lower than in other months. This might be related to the fact that in those months, the temperature is lower compared with other months, so other meteorological parameters, such as wind speed and wind direction may have a more dominant effect on the ETMH than in other months.

Although in general surface temperature has a large impact on the mixing layer, other factors play a leading role in some cases. Then the relationship between the ETMH and temperature is low. For instance, the value is -0.818 in 2, Dec. 2007, which illuminates that the ETMH variation is opposite to temperature, and other meteorological factors are the dominant ones in this period.

4.2 Correlation between the ETMH and surface wind speed

Wind Speed (WS) is found to be another important factor impacting the MH. Similar to the correlation analysis between the ETMH and temperature, that of ETMH and WS is calculated and analyzed. Table 3 shows the results of the correlation retrieved between both quantities. The correlation coefficients are highest for winter indicating that the wind speed plays a dominant role in seasons with little solar irradiation.

The box graph of the correlation coefficients between ETMH and WS is also shown in Fig 8. We can see in this graph, that all the means are in the range of 0.22 and 0.54, much lower than those between ETMH and temperature. The median ranges from 0.24 to 0.72, the maximum median occurs in April. The dynamic range is larger than that between the ETMH and temperature, which indicates that in some cases, wind can dominate the ETMH, but this does not happen frequently. This also can be seen from the difference of maximum and minimum in each month.

In contrast to the correlation between the ETMH and temperature, the correlation between the ETMH and wind speed in the cold season is in general larger than in the warm season. This

indicates that in winter WS has a stronger effect on the ETMH than in summer.

On the basis of the correlation analyses, different days can be classified with respect to four situations: a) both temperature and WS show good correlation with the ETMH, as for instance on 8 May, 29 Nov., 13 May; b) correlation of the ETMH with temperature is high, but with WS is rather low, as for instance on 14 May, 9 Nov., 22 Nov.. The occurrence of cases a) and b) are quite frequent; c) correlation of the ETMH with WS is high, but with temperature is rather low, as for instance on 2 Dec.. This case hardly appeared; d) Not only temperature but also WS is irrelevant to the ETMH, as for example on 7 Dec. and 8 Dec.. Also the probability for case d) is very small. For these cases, other factors than temperature and WS, for example wind Direction (WD), relative humidity (RH) and pressure(p), might play a dominant role.

4.3 Influence of atmospheric lifetime on the determination of the ETMH

The proposed method to determine the ETMH depends on two major assumptions. Firstly, it's on the occurrence of an effective mixing of pollutants throughout the whole mixing layer. Secondly, it's on the fact that the local conditions are not significantly affected by pollutants from distant sources. The second assumption might not be fulfilled especially during winter time, because usually a) higher wind speeds appear and b) the NO_x lifetime becomes substantially longer. Under such conditions distant sources can have a strong influence on our new method. To investigate these effects in more detail, we selected the period from 6 Jan. to 10 Jan.. Fig 9 describes the variation of the ETMH, temperature, WS, RH and pressure from 6 Jan. to 10 Jan..

During the first part of the selected period unrealistically high ETMH were observed. For these observations, temperature was low and wind speed rather high. We also calculated back trajectories [http://www.ready.noaa.gov/hysplitarc-bin/traj1file.pl?metdata=GDAS1] (see Fig. 10) and found that for 6 to 8 January the air masses came indeed from polluted sources.

In contrast, on 9 and 10 January, the air masses traversed the ocean before they arrived over the measurement site (see Fig. 10). Thus they carried less pollution compared to the period from 6 to 8 January. Together with the data on WS and WD we thus can explain the reason why the ETMH of the first days is larger than on the following days. The observations in January 2007 indicate a general limitation of our method, which is most pronounced in winter. Under such conditions, the passive DOAS might observe NO_2 at higher altitude, which is transported from distant sources but which can not be observed by the active DOAS. This effect will lead to an overestimation of the ETMH according to equation 1

4.4 Comparison with other results

In a resent analysis covering 15 years from 1990 to 2004, Yang et al. presented of MH variation determined in Shanghai at 2:00, 8:00, 14:00 and 20:00 [Yang et al. 2006]. In their study, daily ML were calculated based on atmospheric stability and wind speed on the surface (10m above ground) according to the national standard (GB/T 13201-91) of China, all the raw data come from official data of Shanghai Meteorological Bureau . Unfortunately, there is no temporal overlap between their results and our observations. However, since Yang's results are 15 years averages, they can be considered as representative of the seasonal variation of the ETMH in Shanghai. In Fig.3, we compare the monthly average ETMH with their results.

The ETMH derived from the DOAS observations is nearly 22% lower than the mean ML at 8:00,

but it is about 14% larger at 14:00. However, it should be noted that in Yang's results also substantial differences are found for different years: the minimum of the MH appeared in 1995 (0.57km at 8:00 and 0.82km at 14:00), while the maximum appeared in 2004 (0.68km and 0.91km at 8:00 and 14:00 respectively).

Taking into account that the ETMH and ML are derived by two completely different methods, the differences between both data sets are rather small.

Fig 11 shows the annually averaged daily variation of the ETMH from 7:00 to 16:00 in 2007 (A). The maximum of the ETMH occurs at 14:00. This is similar to the results from Yang et al.(B).

In Fig.12, The comparison of DOAS result with MESSy(Modular Earth Submodel System, [J¨ockel et al., 2006]) shows the correlation is high as expected, it's 0.693 in October and 0.872 in December, but DOAS result is 0.127km, about 23%, higher than MESSy in October and 0.134km, about 29%, higher in December. But here it should be mentioned that the MESSy result is calculated in 2006, our measurement is carried out in 2007.

To compare the DOAS-derived ETMH, we added the 3-hourly boundary layer depth determined by NCEP's GDAS (Global Data Assimilation System) model (ARL, http://ready.arl.noaa.gov/READYamet.php), which were made at the same location (31.30, 121.50) during the DOAS operations. Considering limited ETMH values in March, June and October, we left those data out of account. The correlation values between the ETMH and boundary layer depth at 8:00, 11:00 and 14:00 (overlap time) in Fig 13 were 0.547, 0.554 and 0.631, respectively, showing a steady increasing correlation and a small standard deviation along the time. Consequently, the better agreement found in the afternoon suggested that the DOAS method might prove satisfactory to estimate the mixing height when it is fully developed. The monthly correlation coefficients between ETMH and boundary layer depth in Fig 14 ranged between 0.627 and 0.859, highest in December, which was in accordance with comparison of DOAS with MESSy. Fig.15 depicted monthly ETMH and boundary layer depth in 2007 and the percentage difference between them ranged from 4% to 35%. It is well known that MH in winter is low because of weaker solar radiation, but the boundary layer depth in Nov and Dec were higher than other months shown in Fig15**,** which implied these two month results might contain some errors. Through above comparison between these two different methods, it was suggested that DOAS-derived ETMH can be considered reliable.

5. Errors of the method

Errors of the ETMH derived from the combination of active DOAS and passive DOAS origin from uncertainties of the assumed NO_2 vertical distribution profile and measurement errors of the two instrument themselves.

As shown in Fig 1, our method is based on the assumption of a specified vertical profile; in our case a constant NO_2 concentration was assumed. Of course, the real profile will in general differ from this assumed profile. An additional, but associated error results from the fact that the passive DOAS detects NO_2 not only in the mixing layer but also in the free troposphere. If considerable NO_2 exists in free troposphere, it will be erroneously regarded as being in the mixing layer. Consequently, this effect leads to an overestimation of the retrieved ETMH. Suppose that the NO_2 concentration in the free troposphere is 2% of that in the mixing layer and that the free troposphere

is five times as high as the mixing layer. The resulting error of the retrieved ETMH according to equation 3 would be 10%. As mentioned above, if temperature in winter is low and wind comes from inland high-polluted areas, it will bring NO_2 to Shanghai, part of it might be present at high altitudes in the free troposphere. This can lead to a strong overestimation of the real ETMH (see section 4.3).

If the concentration of NO_2 is small, measurement errors of the instruments themselves can become the dominating error source. The uncertainty of the passive DOAS instrument is about > 50% for NO_2 VCDs < $0.5*10^{16}$ molec/cm². That means that for VCD_{ETMH} in that range or below, the uncertainties of the method becomes larger than 50%. Note, however, that in Shanghai, typical VCD_{ETMH} are by far larger and the respective errors are smaller [Chen et al.,2009].

Similarly, also for low surface concentrations derived from the active DOAS, the uncertainties of the ETMH increase, since this quantity appears in the denominator of equation 1. This might become especially important if a systematic bias exists for the data from the active DOAS. For low values of the analysed surface concentrations, even small systematic biases can lead to strong systematic deviations of the derived ETMH. This might be one potential reason for the rather high values of the ETMH in May (see Fig. 5). In those months many observations of the active DOAS yielded rather small surface concentrations of NO_2.

In addition to vertical gradients of the NO_2 concentration within the mixing layer, also horizontal gradients affect the retrieval. If, for example, an air mass with higher NO_2 concentration emerges at low altitude over the measurement site, it will increase the results of the active DOAS leading to an underestimation of the MH. However, since in this study hourly averages are used, this effect should be rather small.

6 Conclusions

We introduced a new method for the determination of the mixing layer height by combination of active DOAS and passive DOAS observations of NO_2. In contrast to conventional definitions of the mixing layer height, our method is sensitive to the vertical distribution of trace gases; thus we refer to the retrieved layer height as an 'effective trace gas mixing height' (ETMH). Depending on the atmospheric lifetime and vertical exchange, the ETMH could differ systematically from the meteorological mixing layer height. However, for several applications, the ETMH might be a well suited quantity, especially for studies with focus on the dispersion and transport of pollutants.

We analyzed trace gas observations in Shanghai over one year (1017 hourly means in 93 days in 2007), and found the ETMH to range between 0.1km and 2.8km (average is 0.78km); more than 90% of the measurements yield an ETMH between 0.2km and 2.0km. The seasonal and diurnal variation of the ETMH shows good agreement with mixing layer heights derived from meteorological observations [Yang et al. 2006].

Finally, we investigated the relationship of the derived ETMH to temperature and wind speed and found correlation coefficients of 0.65 and 0.37, respectively. Also the wind direction has an impact on the measurement to some extent. Especially in cases when the air flow comes from highly polluted areas and the atmospheric lifetime of NO_2 is long (e.g. in winter), the NO_2 concentration at high altitudes over the measurement site can be enhanced, which leads to an overestimation of the ETMH. Enhanced NO_2 concentrations in the free atmosphere and heterogeneity within the mixing layer can cause additional uncertainties.

Acknowledgements

We thank the National High-tech R&D Program of China and NSFC for supporting this research. We also acknowledge Chen Dan's former research work for this study.

References

A.FEBO, C.PERRINO, I.ALLEGRINI: MEASUREMENT OF NITROUS ACID IN MILAN, ITALY, BY DOAS AND DIFFUSION EDNUDERS[J], Atmos. Environ.,30(21), 3599-3609, 1996

A.C.Vandaele, C. Fayt, F. Hendrick, C. Hermans, F. Humbled, M. Van Roozendael, M. Gil, M. Navarro, O. Puentedura, M. Yela, G. Braathen, K. Stebel, K. Tørnkvist, P. Johnston, K. Kreher, F. Goutail, A. Mieville, J.-P. Pommereau, S. Khaikine, A. Richter, H. Oetjen, F. Wittrock, S. Bugarski, U. Frie, K. Pfeilsticker, R. Sinreich, T. Wagner, G. Corlett, R. Leigh: An intercomparison campaign of ground-based UV-visible measurements of NO_2, BrO, and OClO slant columns: Methods of analysis and results for NO2, J. Geophys. Res., Vol.110, D08305, doi:10.1029/2004JD005423, 2005

Berman, S., Yeong, J. K., Zhang, J., and Rao, T.: Uncertainties in estimating the mixing depth–comparing three mixing-depth models with profiler measurements, Atmos. Environ, 31, 3023– 3039, 1997

D. Chen, B. Zhou, S. Beirle,L. M. Chen, and T. Wagner: Tropospheric NO_2 column densities deduced from zenith-sky DOAS measurements in Shanghai, China, and their application to satellite validation, Atmos. Chem. Phys., 9, 3641–3662, 2009

F.Evangelisti, A.Baroncelli, P.Bonasoni, G.Giovanelli; F. Ravegnani,: Differential optical absorption spectrometer for measurement of tropospheric pollutants, APPLIED OPTICS, 34(15), 2737-2744, 1995

K. Kourtidis*, I. Ziomas, C. Zerefos, A. Gousopoulos, D. Balis, P. Tzoumaka: Benzene and toluene levels measured with a commercial DOAS system in Thessaloniki, , Atmos. Environ., 34.1471-1480, 2000

Hönninger, G. and Platt, U.:The role of BrO and its vertical distribution during surface ozone depletion at Alert, Atmos. Environ., 36, 2481–2489, 2002

J¨ockel, P., Tost, H., Pozzer, A., Br¨uhl, C., Buchholz, J.,Ganzeveld, L., Hoor, P., Kerkweg, A., Lawrence, M. G.,Sander, R., Steil, B., Stiller, G., Tanarhte, M., Taraborrelli, D.,van Aardenne, J., and Lelieveld, J.: The atmospheric chemistry general circulation model ECHAM5/MESSy1: consistent simulation of ozone from the surface to the mesosphere, Atmos. Chem. Phys., 6, 5067–5104, 2006,

M. A. García, M. L. S´anchez, B. de Torre, and I. A. Pérez: Characterisation of the mixing height temporal evolution by means of a laser dial system in an urban area – intercomparison results with a model application, Ann. Geophys., 25, 2119–2124, 2007

M. Bruns, S. A. Buehler, J. P. Burrows, A. Richter, A. Rozanov, P. Wang, K. P. Heue, U. Platt, I. Pundt, and T. Wagner: NO2 Profile retrieval using airborne multi axis UV-visible skylight

absorption measurements over central Europe. Atmos. Chem. Phys.,6, 3049–3058, 2006

Noxon, J. F.:Nitrogen dioxide in the stratosphere and troposphere measured by ground-based absorption spectroscopy, Science, Vol.189, No.4202,547–549, 1975.

Seibert P., Beyrich F., Gryning S.-E.S.-E., Joffre S.,Rasmussen A., Tercier P: Review and intercomparison of operational methods for the determination of the mixing height, Atmos. Environ.,Vol. 34, No.7, 1001-1027,2000

Perner, D., and U. Platt:Detection of nitrous acid in the atmosphere by differential optical absorption, *Geophys. Res. Lett.* 6 ,917–920, 1979

Platt U: Differential optical absorption spectroscopy (DOAS), in Air monitoring by spectroscopic techniques. Chem. Anal Seri, 127, edit by Markus W. Sigrist,27-84, 1994

U. Platt , J. Stutz: Differential Optical Absorption Spectroscopy -Principles and Applications, Springer, 2008.

Qi F., Liu W.Q., Zhou B., Li Z.B., Chui Y.J.: Improving DOAS System Measurement Precision with Artificial Neutral Network Method, ACTA OPTICA SINICA, 22(11), 1346－1349, 2002

Solomon, S., Portmann, R. W., Sanders, R. W., J. S. Daniel, W. Madsen, B. Bartram, E. G. Dutton:On the role of nitrogen dioxide in the absorption of solar radiation, J. Geophys. Res., 104(D10), 12047–12058, 1999.

Stutz 2006，S.Wang, R. Ackermann, and J. Stutz，Vertical profiles of O3 and NOx chemistry in the polluted nocturnal boundary layer in Phoenix, AZ: I. Field observations by long-path DOAS，Atmos. Chem. Phys., 6, 2671–2693, 2006

Stutz 2004，Vertical profiles of NO3, N2O5, O3, and NOx in the nocturnal boundary layer: 1. Observations during the Texas Air Quality Study 2000 JOURNAL OF GEOPHYSICAL RESEARCH, VOL. 109, D12306, doi:10.1029/2003JD004209, 2004

Yang Y. J.,Tan J.G., Zheng Y.F., Cheng S.H.: STUDY ON THE ATMOSPHERIC STABILITIES AND THE THICKNESS OF ATMOSPHERIC MIXED LAYER DURING RECENT 15 YEARS IN SHANGHAI, SCIENTIA METEOROLO GICA SINICA, 26(5), 537－541, 2006

Yu, Y., Geyer, A., Xie, P., Galle, B., Chen, L. M., and Platt, U.: Observations of carbon disulfide by differential optical absorption spectroscopy in Shanghai, Geophys. Res. Lett., 31, L11107, doi:10.1029/2004GL019543, 2004.

Zhou B., Hao N., Chen L.M.: A study on the effect of Fraunhofer structure on the measurement of atmospheric pollutants with differential optical absorption spectroscopy, Acta Physica Sinica,9, 4445-4450, 2005

Zhou B., Liu W.Q., Qi F. Li Z.B., Chui Y.J., Error analysis in Differential Optical Absorption Spectroscopy, ACTA OPTICA SINICA, 22(8), 957-961, 2002

Table1: number of measurement days in each month

	Jan	Feb	Mar	Apr	May	Jun	Sep	Oct	Nov	Dec
days	7	12	4	15	12	3	7	8	15	10

Table2: Correlation of ETMH with surface temperature and wind speed for different seasons.

Season	Correlation coefficient of ETMH and T	Correlation coefficient of ETMH and WS
Spring	0.59	0.43
Summer	0.7	0.38
Autumn	0.81	0.22
winter	0.68	0.48

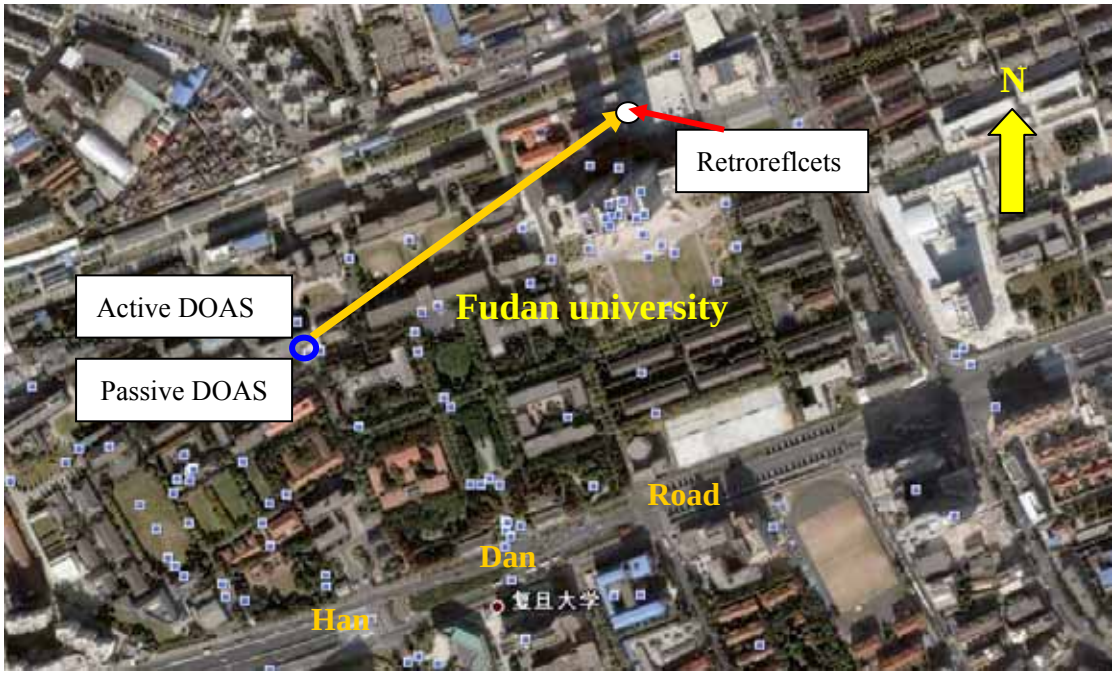

Fig. 1 Measurement site, active and passive are located in Fudan University, Shanghai, China, light path of active DOAS is 507m.

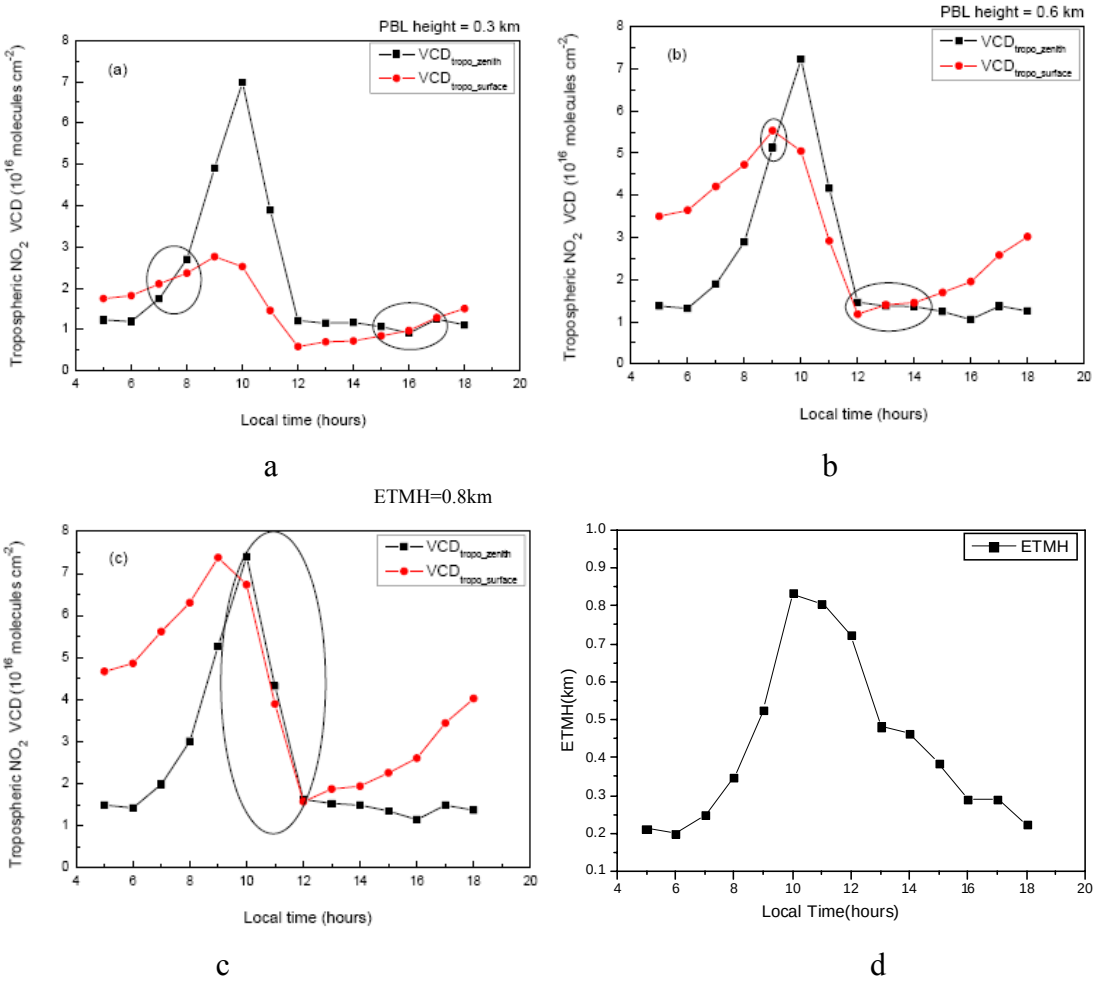

Fig. 2. a, b and c, the comparison of VCD_{ETML} results of active DOAS and passive DOAS for different ETMH assumptions at different time on 9, June, 2007 (Chen et al.,2009), d is the diurnal variation of ETMH calculated by the assumption in this particular day.

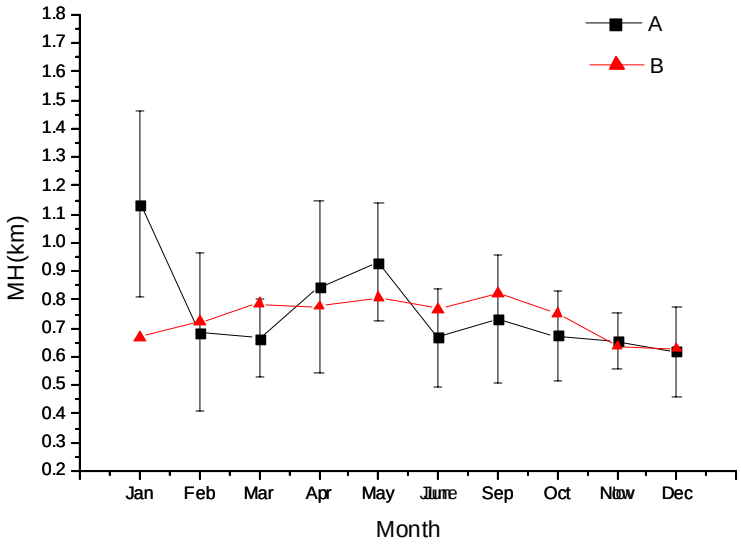

Fig 3: A) Monthly average ETMH in 2007. The error bars indicate the standard variation. Note that the high values in January overestimate the true values because of the long lifetime of tropospheric NO_x in winter (see section 4.3). B) Monthly average MH derived from meteorological data at 8:00 and 14:00 local time.[Yang et al., 2006].

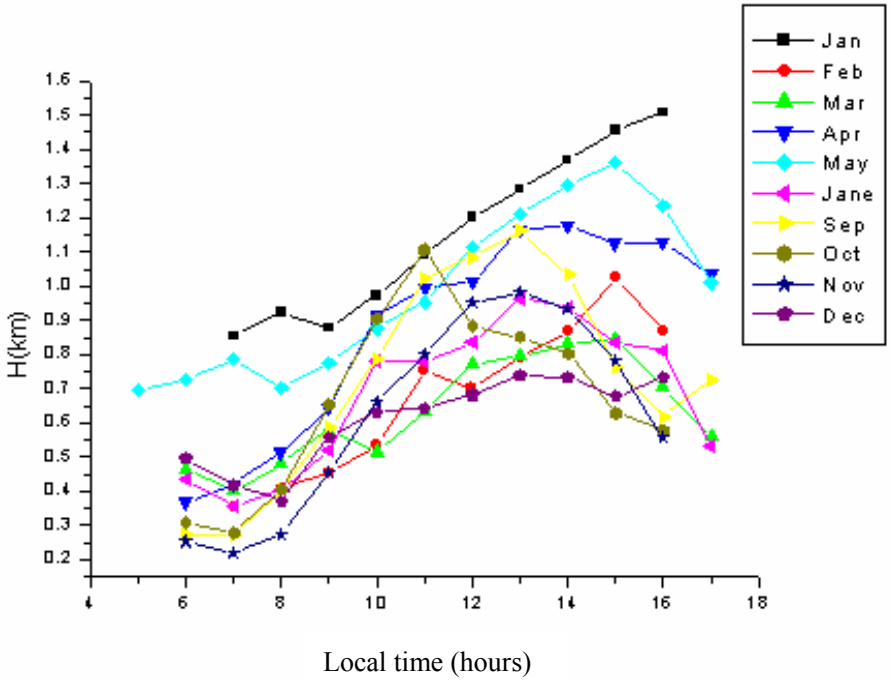

Fig. 4 Monthly averaged diurnal variation of the ETMH. Again it should be noted that the high values in January overestimate the true ETMH (see section 4.3).

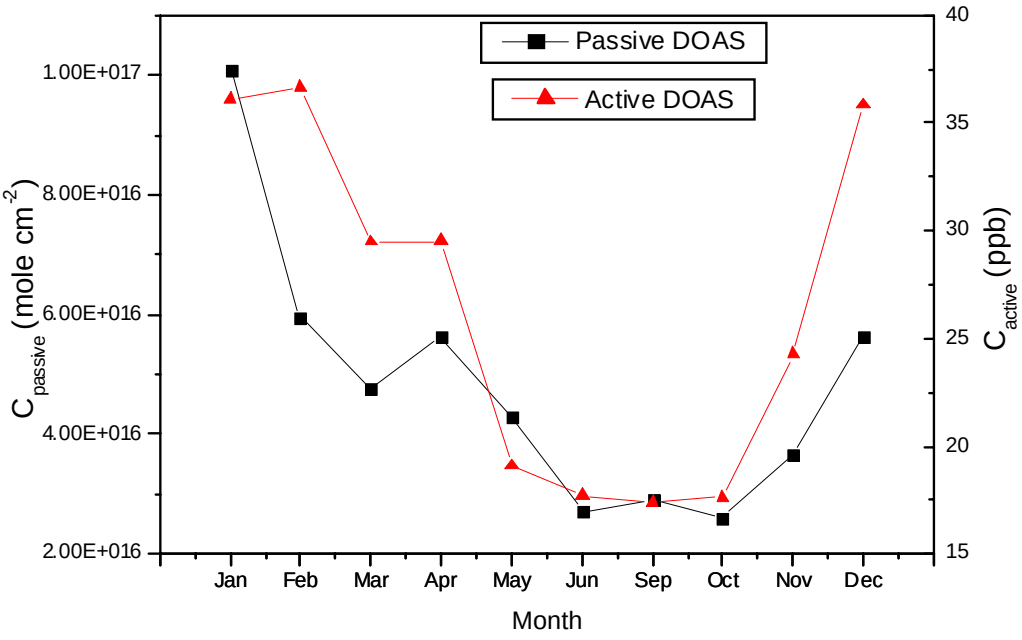

Fig.5 Monthly average of passive DOAS and active DOAS in 2007, it could be seen both measurements have high concentration in winter and low concentration in summer, because of the lifetime of NO2 in atmosphere.

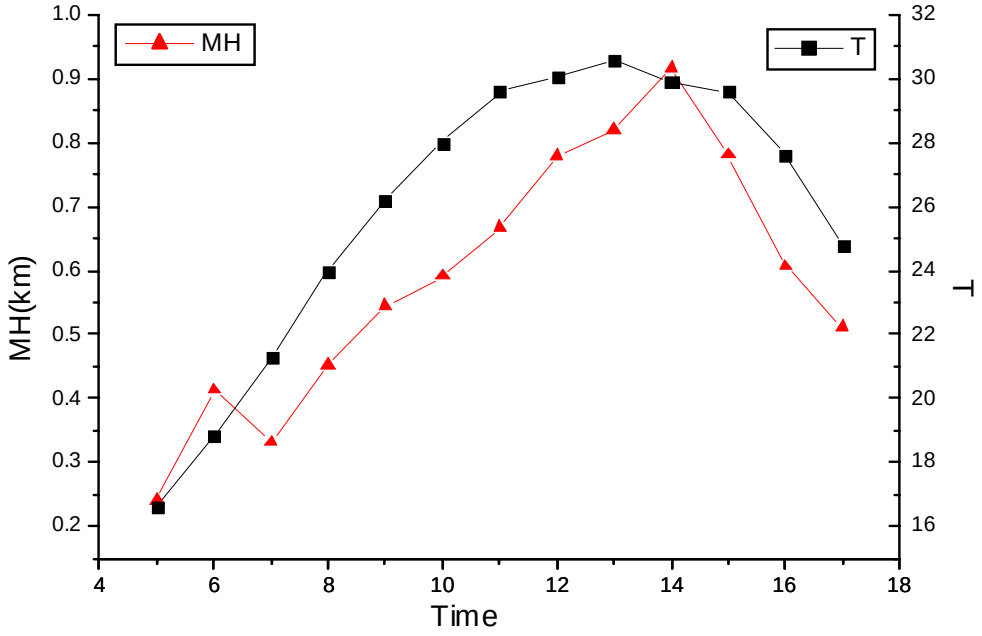

Fig6.a

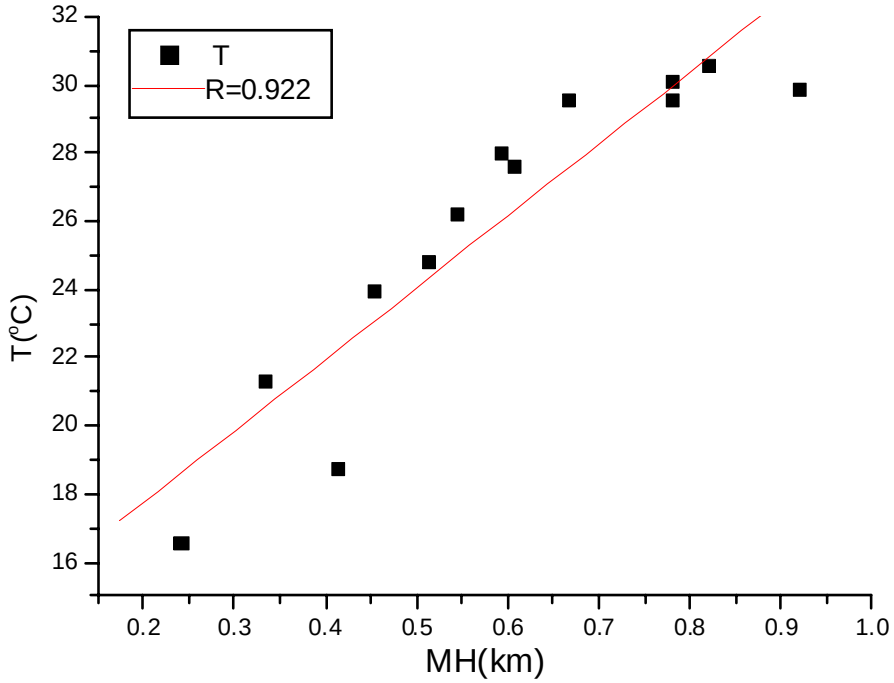

Fig6.b

Fig 6: Correlation between the ETMH and surface temperature on 11, May, 2007.

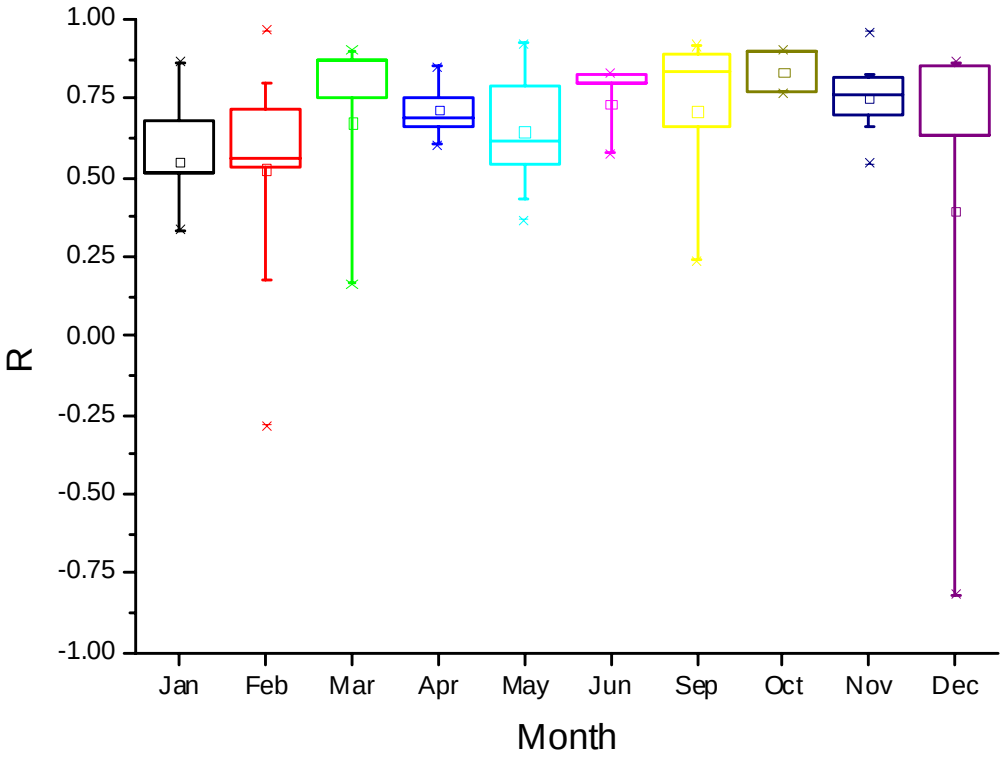

Fig 7: Monthly variations of the correlation between the ETMH and surface temperature, in Fig. different color corresponding to different month

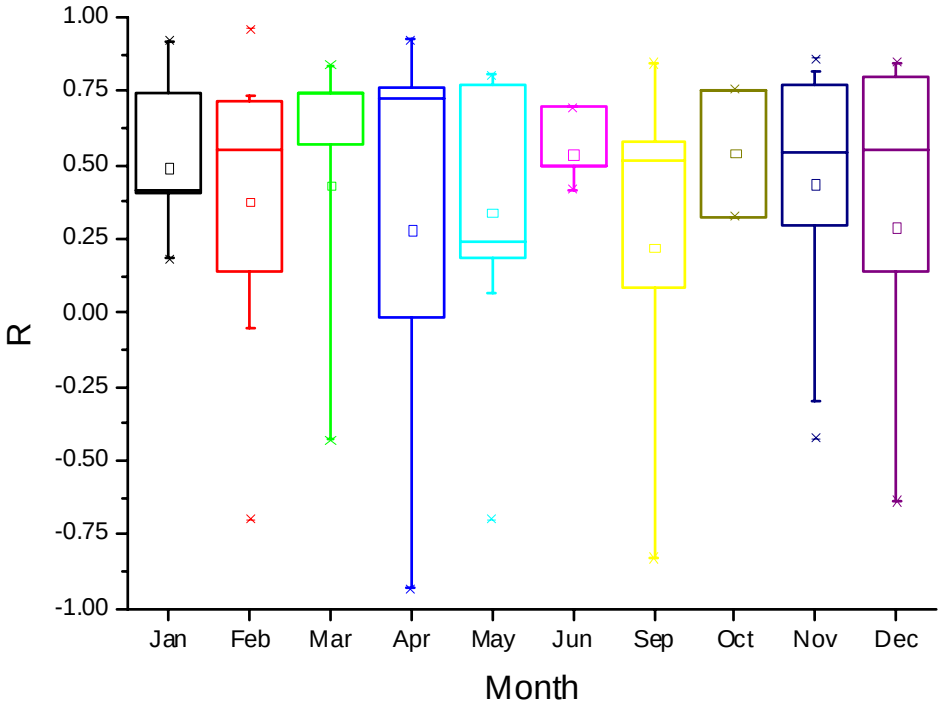

Fig 8: Monthly variations of the correlation between the ETMH and wind speed, in Fig. different color corresponding to different month

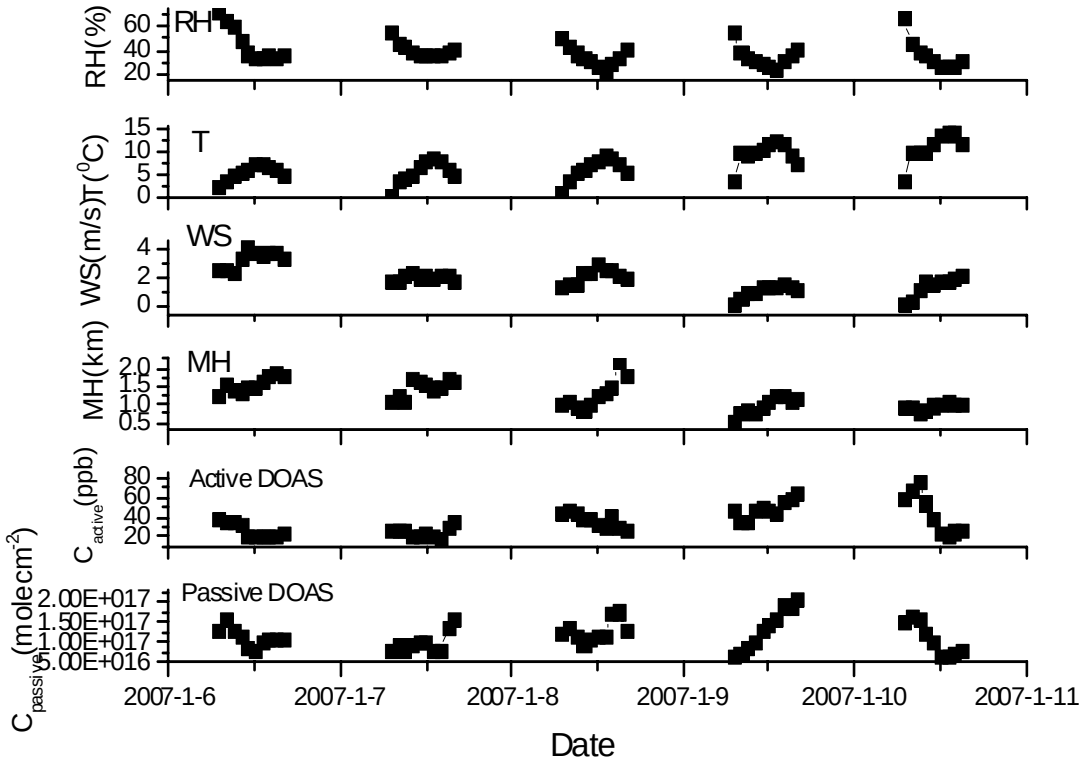

Fig. 9: Variation of the $C_{passive}$, C_{active}, ETMH, temperature, WS, RH and pressure from sixth to tenth of January. The ETMH in Jan. 6, 7, 8 is obviously higher than in Jan. 9 and 10,. This phenomenon conflicts with the expectation that both the MH and its variation is low in winter, potential reason for this please see Sect. 4.3 in text .

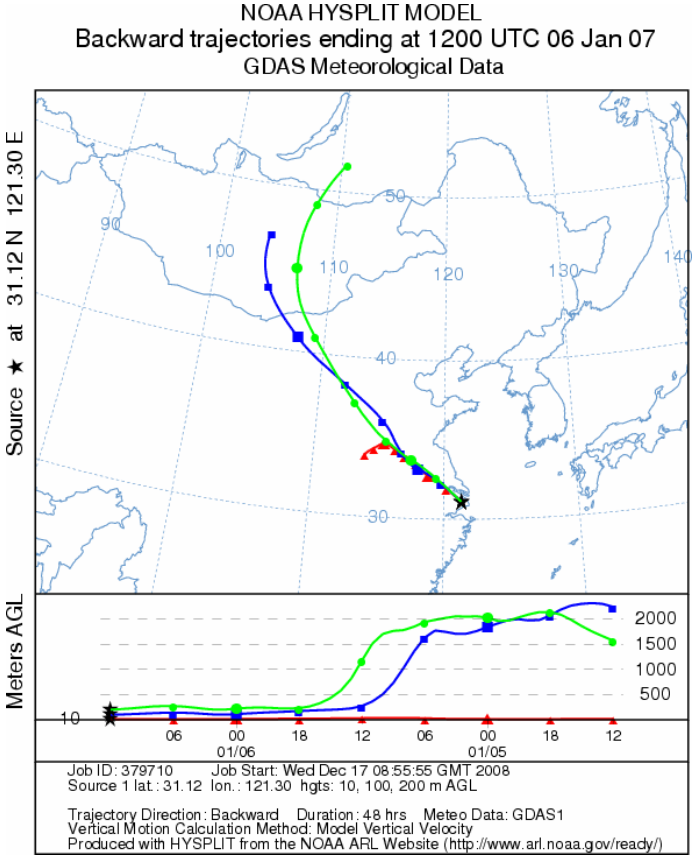

Fig10.a

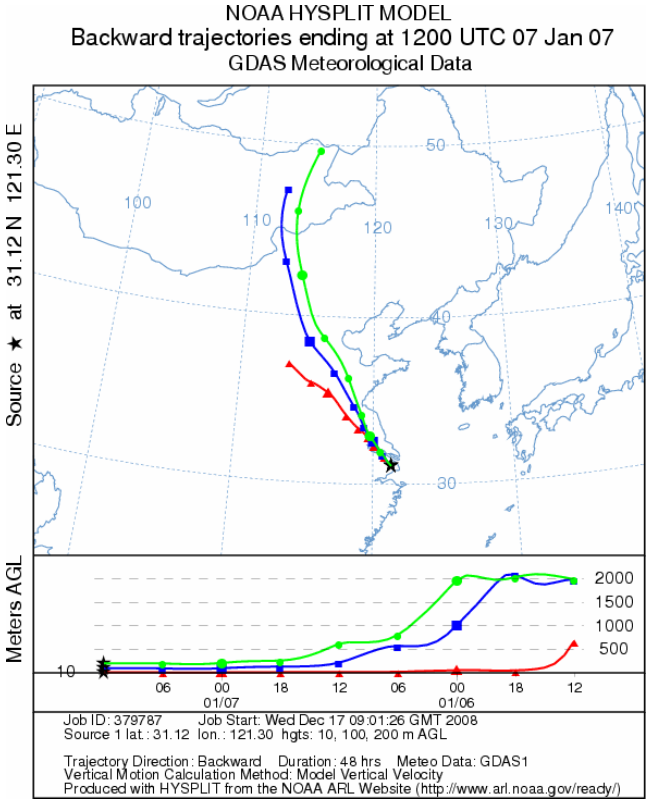

Fig10.b

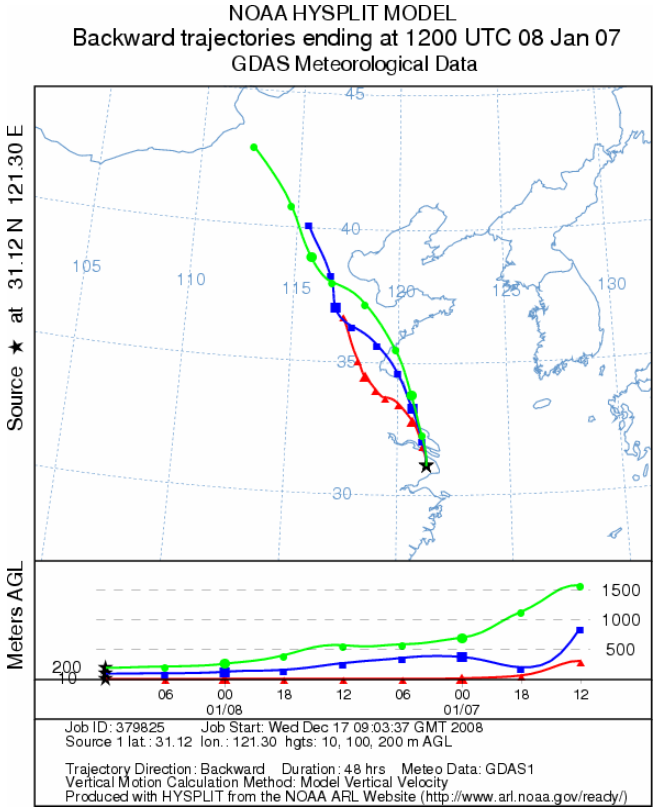

Fig10.c

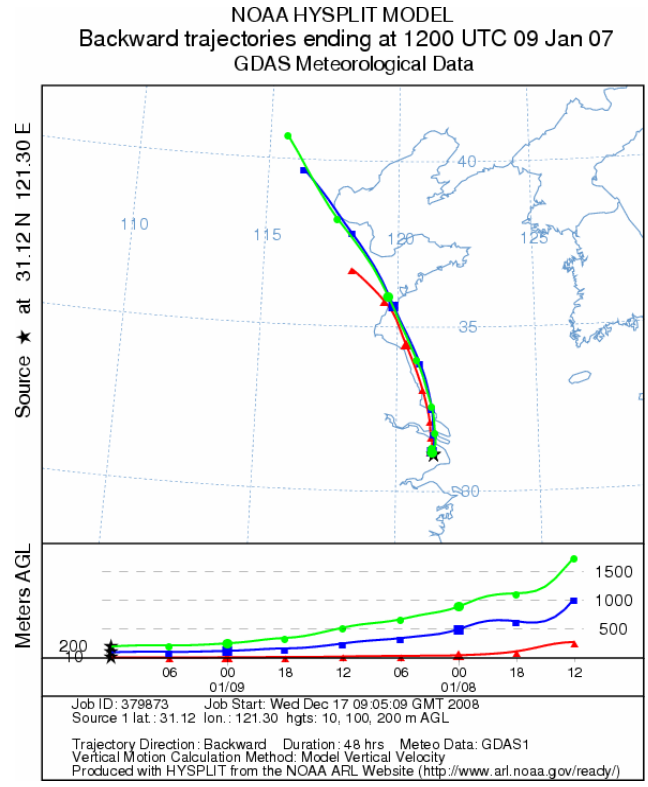

Fig10.d

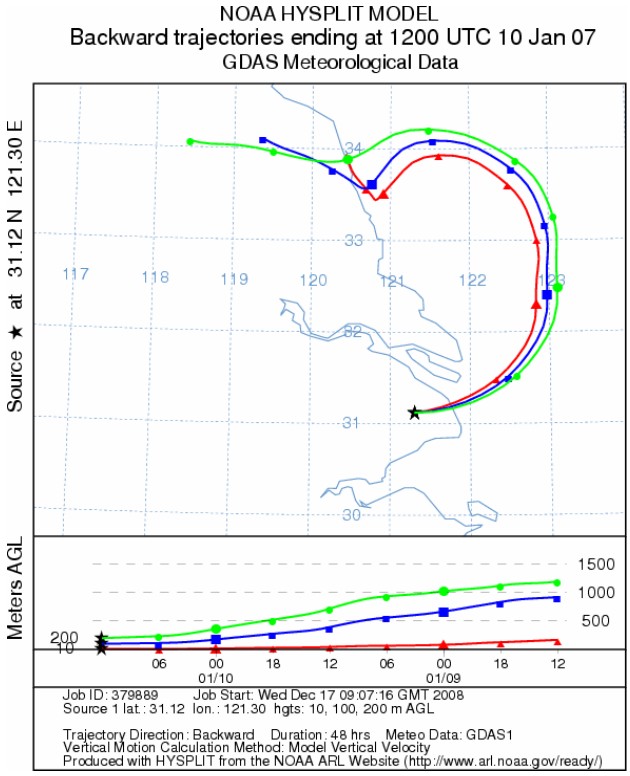

Fig10.e

Fig. 10: Back trajectories (48 h) arriving in Shanghai from sixth to tenth (a to e), January.

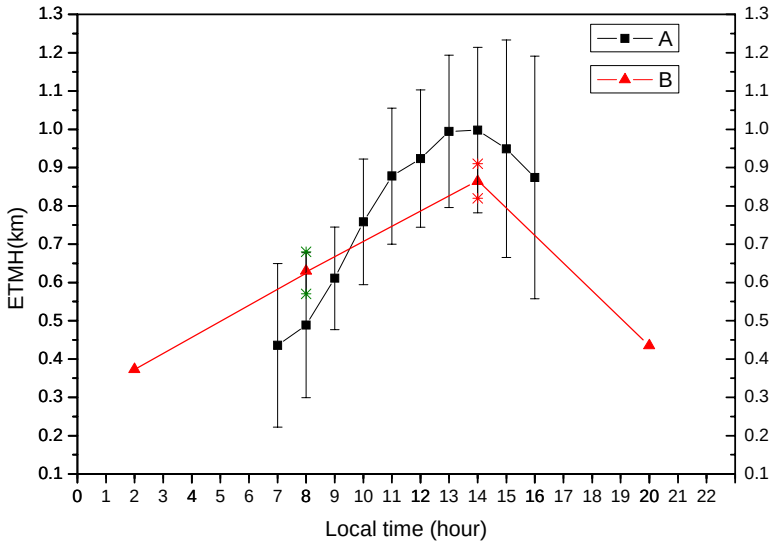

Fig 11: Annually averaged daily variation of the ETMH in 2007 (A) and 15 years MH variation at 2:00, 8:00 (including min, max value), 14:00 (including min, max value) and 20:00 from 1990 to 2004 in Shanghai (B).

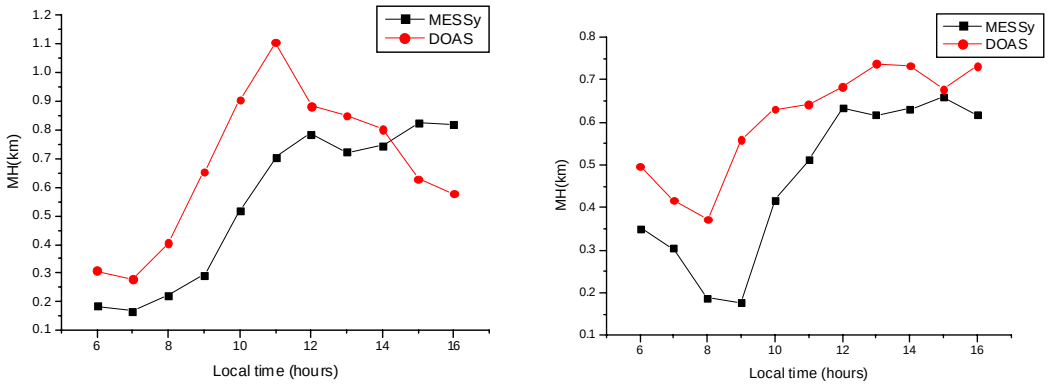

a October b December

Fig.12 The comparison of MESSy and DOAS result shows the correlation is high as expected, it's 0.693 in October and 0.872 in December, but DOAS result is 0.127km, about 23%, higher than MESSy in October and 0.134km, about 29%, higher in December.

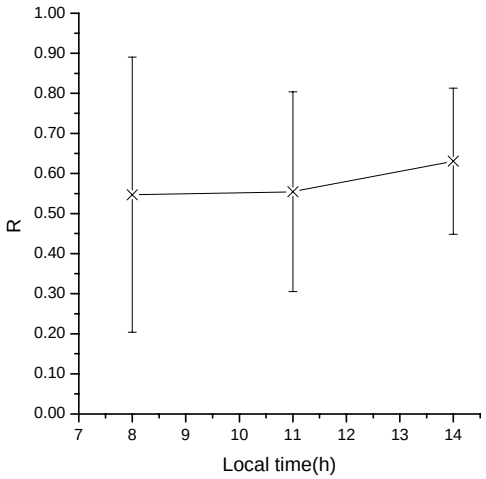

Fig.13 Correlation variations between the ETMH and boundary layer depth at 8:00, 11:00 and 14:00. The error bars indicate the standard deviation.

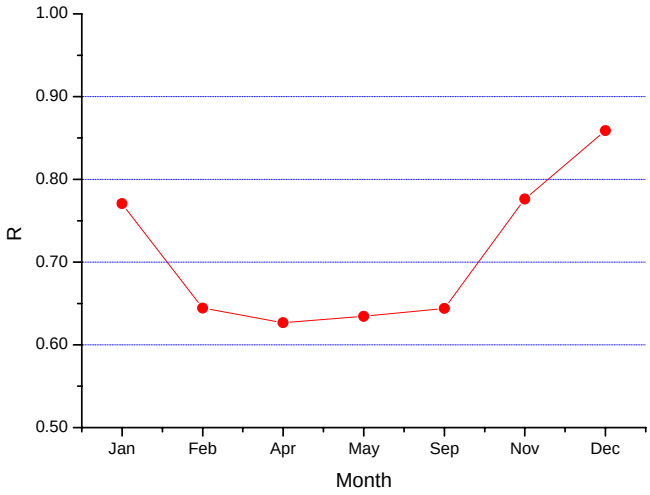

Fig.14 Monthly variations of the correlation between ETMH and boundary layer depth.

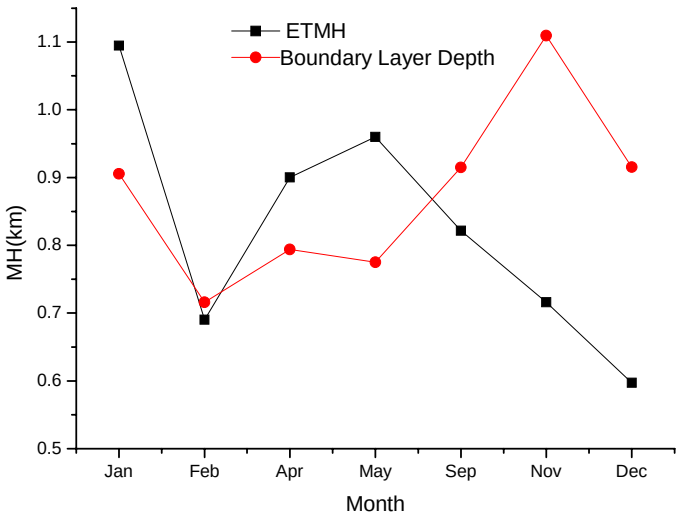

Fig.15 Monthly ETMH and boundary layer depth in 2007(only including8:00, 11:00 and 14:00 values)